The EMBO Journal (2013) 32, 713–727
www.embojournal.org

TRANSPARENT PROCESS

THE EMBO JOURNAL

Rac and Rab GTPases dual effector Nischarin regulates vesicle maturation to facilitate survival of intracellular bacteria

Coenraad Kuijl[1,5,*], Manohar Pilli[1,2,5], Suresh K Alahari[3,5], Hans Janssen[4], Poh-Sim Khoo[1], Karen E Ervin[1], Monica Calero[1], Sobhanaditya Jonnalagadda[2], Richard H Scheller[1], Jacques Neefjes[4] and Jagath R Junutula[1,*]

[1]Genentech Inc., South San Francisco, CA, USA, [2]Department of Biochemistry, University College of Science, Osmania University, Hyderabad, India, [3]Department of Biochemistry and Molecular Biology, Louisiana State University Health Sciences Center, New Orleans, LA, USA and [4]Division of Cell Biology, The Netherlands Cancer Institute, Amsterdam, The Netherlands

The intracellular pathogenic bacterium *Salmonella enterica* serovar typhimurium (*Salmonella*) relies on acidification of the *Salmonella*-containing vacuole (SCV) for survival inside host cells. The transport and fusion of membrane-bound compartments in a cell is regulated by small GTPases, including Rac and members of the Rab GTPase family, and their effector proteins. However, the role of these components in survival of intracellular pathogens is not completely understood. Here, we identify Nischarin as a novel dual effector that can interact with members of Rac and Rab GTPase (Rab4, Rab14 and Rab9) families at different endosomal compartments. Nischarin interacts with GTP-bound Rab14 and PI(3)P to direct the maturation of early endosomes to Rab9/CD63-containing late endosomes. Nischarin is recruited to the SCV in a Rab14-dependent manner and enhances acidification of the SCV. Depletion of Nischarin or the Nischarin binding partners—Rac1, Rab14 and Rab9 GTPases—reduced the intracellular growth of *Salmonella*. Thus, interaction of Nischarin with GTPases may regulate maturation and subsequent acidification of vacuoles produced after phagocytosis of pathogens.

The EMBO Journal (2013) **32,** 713–727. doi:10.1038/emboj.2013.10; Published online 5 February 2013
Subject Categories: membranes & transport; microbiology & pathogens
Keywords: Nischarin; Rab14; Rab9; Rac1; *Salmonella*

*Corresponding authors. JR Junutula or C Kuijl, Research and Development, Genentech Inc., 1 DNA Way, South San Francisco, CA 94080, USA. Tel.: +1 650 225 4533; Fax: +1 650 742 1580; E-mail: jagath@gene.com or Tel.: +1 650 467 8319; Fax: +1 650 742 1580; E-mail: kuijlc@gene.com
[5]These authors contributed equally to this work.

Received: 21 November 2012; accepted: 8 January 2013; published online: 5 February 2013

Introduction

Salmonella species are facultative intracellular bacterial pathogens causing a variety of enteric diseases in vertebrates worldwide. *Salmonella enterica* serovar typhimurium is the causative agent of debilitating gastroenteritis in humans. *Salmonella* gains entry to the intracellular milieu of the body via trans-endocytosis by microfold (M) cells (Kohbata *et al*, 1986; Jones *et al*, 1994) and subsequent uptake by macrophages, B cells (Souwer *et al*, 2009) or dendritic cells present in the lamina propria (Rescigno *et al*, 2001). These phagocytic cells are exploited by *Salmonella* as vehicles to disseminate itself throughout the host body. To enhance uptake in phagocytic cells (Lombardi *et al*, 1993; Pavlova *et al*, 2011) and to induce uptake in non-phagocytic cells, *Salmonella* secretes effector proteins into the host cell via the type 3 secretion system (T3SS) encoded by *Salmonella* pathogenicity island 1 (SPI-1) (Lostroh and Lee, 2001). After uptake and acidification (Yu *et al*, 2010) of the *Salmonella*-containing vacuole (SCV), *Salmonella* secretes effectors encoded by the *Salmonella* pathogenicity island 2 (SPI-2) act to create and maintain the replicative niche (Hensel *et al*, 1998; Haraga *et al*, 2008). During this process, the SCV serially acquires early endosomal markers (e.g., EEA1 and transferrin receptor) (Steele-Mortimer *et al*, 1999b) followed by late endosomal markers (e.g., LAMP) (Garcia-del Portillo *et al*, 1993; Méresse *et al*, 1999); though the SCV interacts with late endosomes/lysosomes (Drecktrah *et al*, 2007), fusion of SCV with lysosomes is thought to be prevented (Garcia-del Portillo and Finlay, 1995; Rathman *et al*, 1996; Méresse *et al*, 1999; Steele-Mortimer *et al*, 1999a). The various effectors secreted by *Salmonella* orchestrate this acidification, but escape from lysosomal degradation.

Salmonella disrupts the normal pathways of small GTPases like Rac and Rab GTPases, the key regulators of formation, transport and fusion of vesicles in a cell (Zerial and McBride, 2001; Pfeffer, 2003; Palamidessi *et al*, 2008). Two SPI-1 encoded effectors, SopE and SopB, control entry and transport of vesicles by manipulating Rac and Rab GTPases (McGhie *et al*, 2009). SopE activates host Rac GTPase to induce actin remodelling and phagocytosis (Hardt *et al*, 1998). SopB recruits host Rab5 to the phagosomal membrane, stimulating local production of PI(3)P (Mallo *et al*, 2008). SopB also activates the Akt kinase signalling cascade (Steele-Mortimer, 2000). Activated Akt phosphorylates AS160; phosphorylated AS160 dissociates from the membrane. AS160 is a GAP (GTPase activating protein) for Rab14 (Larance *et al*, 2005; Mîinea *et al*, 2005). Dissociation from AS160 enables Rab14 to remain in a membrane-associated active form on the phagosome (Kuijl *et al*, 2007). Here, we identify and characterize Nischarin as a novel dual effector for both Rac and Rab GTPases that regulates the maturation of the SCV. Recruitment of Nischarin

to the SCV via PI(3)P and its sequential interaction with Rab14 and Rab9 leads to acidification of the SCV, creating conditions favourable for intracellular survival of *Salmonella*.

Results

Nischarin is an effector protein of Rab14 GTPase

To understand how intracellular bacteria like *Salmonella* create their replicative niche, and to delineate the role of Rab14 in this process, Rab14-Q70L$_{\Delta C}$, a constitutively active GTP-locked form of Rab14 was used as a bait in a yeast two-hybrid screen of a mouse brain cDNA library. The screen identified Nischarin, a protein previously reported to interact with p21-activated kinases (PAKs), insulin receptor substrate 4 (IRS4), α5 integrin, and the small GTPase Rac1 (Sano *et al*, 2002; Alahari and Nasrallah, 2004; Alahari *et al*, 2004). Nischarin interacted with Rab14-Q70L$_{\Delta C}$, but not with Rab14-S25N$_{\Delta C}$, the GDP-locked mutant (Figure 1A). The GTP-dependent interaction of Nischarin with Rab14 was confirmed by GST bead-binding assays (Figure 1B) and by co-immunoprecipitation (Figure 1C): Nischarin bound strongly to Rab14 in the presence of GMP-PNP, a non-hydrolysable GTP analogue, and to Rab14-Q70L. The endogenous Rab14 and Nischarin proteins could be co-immunoprecipitated by anti-Nischarin antibodies (Supplementary Figure S1A).

Nischarin localizes to endocytic/recycling vesicles (Lim and Hong, 2004). Given that Rab14 also resides partly on early endosomes (Junutula *et al*, 2004), we probed the possible co-localization of Nischarin and Rab14 by immunofluorescence. Rab14 and myc-Nischarin (Figure 1D), as well as endogenous Rab14 and Nischarin (Figure 1E), partly co-localized on vesicles. The extent of co-localization of myc-Nischarin and Rab14 was enhanced by expression of Rab14-Q70L and decreased by expression of a dominant-negative form of Rab14 (Rab14-N124I) (Figure 1D). Nischarin remained membrane associated despite overexpression of GDP-Rab14-N121I, suggesting that Nischarin may localize to endosomes by binding of PI(3)P through its phox homology domain (PXD) (Lim and Hong, 2004). Indeed, treatment of cells with the PI(3)K inhibitor wortmanin or deletion of the PX domain of Nischarin relocalized Nischarin from vesicular structures to the cytosol (Supplementary Figure S1B and C). Moreover, preventing the conversion of PI(3)P to PI(3,5)P_2 with the Pikfyve inhibitor (Jefferies *et al*, 2008) YM201636 increased the number of Nischarin-positive vesicles (Supplementary Figure S1B). In this aspect, Nischarin differs from another Rab14 effector, RUFY1/Rabip4, which, despite the presence of a PIP(3)-binding FYVE motif, can localize to membranes only when complexed with GTP-Rab14 (Yamamoto *et al*, 2010).

A Rab-effector protein typically binds to its cognate Rab GTPases and coordinates various stages of intracellular vesicular transport. Binding of a Rab effector often stabilizes the Rab GTPase in the GTP-bound state by preventing access of a GAP responsible for conversion of the Rab to a GDP-bound form (Jordens *et al*, 2001). Stabilization of a Rab GTPase in the GTP-bound state should be reflected in an increased retention time of the GTPase on the membrane. The effect of Nischarin on Rab14 membrane retention was followed by fluorescent recovery after photo-bleaching (FRAP). Endosomes containing GFP-Rab14 or GFP-Rab5 in the presence or absence of Nischarin were photobleached and monitored for fluorescence recovery to quantify the Rab GTPase cycle of GTP hydrolysis by GAPs and GTP loading by GEF (GTP exchange factor) in living cells. Nischarin quenched recovery of cytosolic Rab14 to the endosomes (Figure 1F). Nischarin did not affect the GTP cycle of Rab5 (Figure 1G) on the same vesicles, indicating a specific interaction between Nischarin and Rab14. The selective effect of Nischarin on the Rab14 GTPase cycle has been observed for other Rab–effector interactions (Jordens *et al*, 2001).

Mapping-specific domains of Nischarin that bind to Rab14 and Rac1 GTPases

We used GST bead-binding assays and yeast two-hybrid analyses to map the domain of Nischarin required for interaction with Rab14. Two truncated derivatives of Nischarin were prepared: one truncation comprising the PXD (Phox homology domain), the LRR (leucine-rich repeat) and the CC (coiled coil) domain collectively called the N-terminal domain (NTD), the other comprising the C-terminal domain (CTD) of unknown function (Lim and Hong, 2004). Rab14-Q70L$_{\Delta C}$ could bind to Nischarin-CTD (aa 1120–1504), but not to Nischarin-NTD (aa 1–1030) (Figure 2A and B; Supplementary Figure S2A). Further deletions of the N-terminal or C-terminal regions of Nischarin-CTD abrogated this interaction (Figure 2A). We then investigated which domain is required for Nischarin recruitment to vesicular membranes. Nischarin-NTD lacking the Rab binding domain

Figure 1 Nischarin is an effector protein of Rab14 GTPase. (**A**) Yeast two-hybrid analysis shows that Nischarin interacts with the GTP-locked form Rab14-Q70L$_{\Delta C}$, but not with the GDP-locked form Rab14-S25N$_{\Delta C}$. The suffix 'ΔC' denotes deletion of the C-terminal CaaX motif (Cys-Gly-Cys) to prevent membrane localization of the Rab GTPase in the yeast cell. (**B**) Western blot of cell lysate of HEK293T cells expressing myc-Nischarin after GST bead-binding assay. Proteins eluted from GST-Rab14 loaded with either GDP or the non-hydrolysable GTP analogue GMP∼PNP were probed with anti-myc antibody (upper panel) and stained with Ponceau S (lower panel) to show equal loading of cell lysates. (**C**) Immunoblot of HEK293T cell lysate containing myc-Nischarin mixed with GFP-Rab14-wt, GFP-Rab14-Q70L or GFP-Rab14-S25N for co-precipitation using anti-myc antibody and probed with anti-GFP antibody (upper panel) or anti-GFP and anti-myc antibody (lower panel). (**D**) Immunofluorescence images of MCF-7 cells showing localization of myc-Nischarin (mouse-anti-myc antibody; secondary Alexa 647 anti-mouse antibody; red) and GFP-Rab14-wt, GFP-Rab14-Q70L or GFP-Rab14-N124I (green). Scale bar = 10 μm. Plot shows extent of co-localization (as mean + s.d.) of fluorescence of myc-Nischarin and GFP-Rab14, GFP-Rab14-Q70L or GFP-Rab14-N124I as measured by the Karl Pearson's coefficient of correlation. *P*-values were obtained with a Student's *t*-test comparing Rab14-N124I with Rab14-WT or Rab14-Q70L ($n > 12$ cells per condition). (**E**) Immunofluorescence images of A172 cells showing localization of endogenous Rab14 (rabbit anti-Rab14 antibody; secondary Zenon Alexa 488 anti-rabbit fab fragment, green) and endogenous Nischarin (Rabbit-anti-Nischarin; secondary Zenon Alexa 647 anti-rabbit fab fragment antibody; red). Scale bar = 10 μm. (**F**) Fluorescence recovery after photobleaching of GFP-Rab14 in the presence or absence of ectopically expressed Nischarin in MCF-7 cells. Endosomes marked by GFP-Rab14 were bleached (laser at 488 nm) and appearance of fluorescence on these vesicles was monitored as a function of time. *P*-value was obtained with F-test comparing FRAP curves of Rab14 with Rab14 + Nischarin, standard deviations are shown ($n > 8$). (**G**) Fluorescence recovery after photobleaching of GFP-Rab5 in the presence or absence of ectopically expressed Nischarin. FRAP experiment was carried out as described above. *P*-value was obtained with F-test comparing FRAP curves of Rab5 with Rab5 + Nischarin. NS indicates no statistical significance ($n > 7$).

was recruited to membranes while Nischarin-CTD remained cytosolic (Supplementary Figure S2B). However, immunofluorescence showed that Nischarin-NTD displayed reduced co-localization with Rab14 in MCF-7 cells (Figure 2C). This indicates that both the interaction with Rab14 and PI(3)P are important for localization of Nischarin to Rab14-positive endosomes.

The situation was different for the other GTPase—Rac1. Both full-length and Nischarin-NTD co-localized on vesicles with GTP-locked Rac1-Q61L (Figure 2D), in agreement with previous findings (Reddig *et al*, 2005). GST bead-binding assays using purified proteins revealed that the GTP-bound and GDP-bound forms of GST-Rac1 could interact with full-length and Nischarin-NTD (Figure 2E). However,

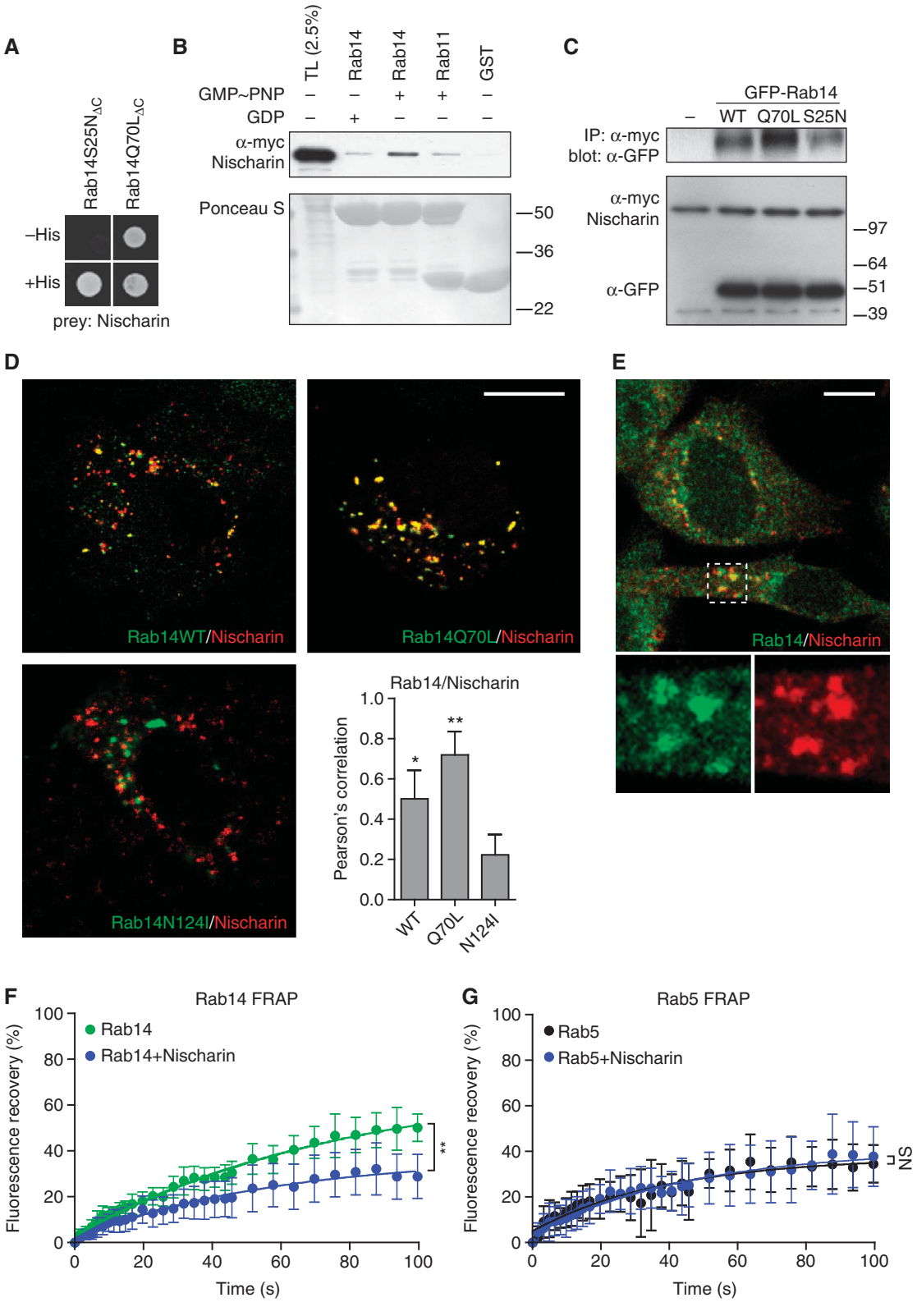

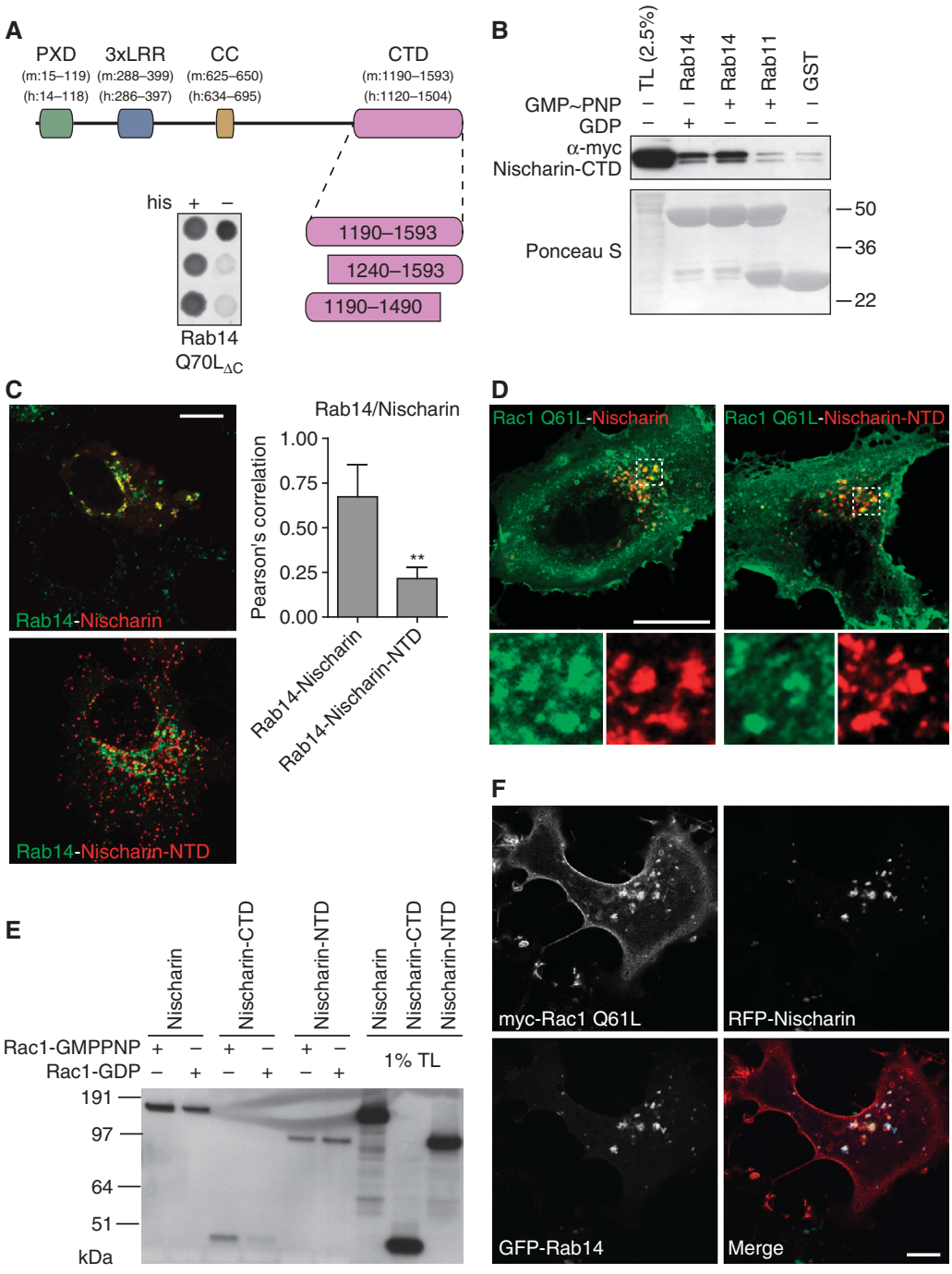

Figure 2 Nischarin domains interacting with Rab14 and Rac1 GTPases. (**A**) Schematic overview of mouse(m) and human(h) Nischarin and mapping of Nischarin binding domain to Rab14. PXD, Phox homology domain; LRRs, leucine-rich repeats; CC, coiled coil; CTD, C-terminal domain. Yeast two-hybrid analysis showing interaction of Rab14-Q70L$_{\Delta C}$ with Nischarin-CTD and its deletion constructs. (**B**) Western blot analysis of proteins eluted from GST-Rab14 beads incubated with myc-Nischarin-CTD in the presence of either GDP or GMP∼PNP and probed with anti-myc antibody (upper panel). Lower panel: Ponceau S staining of the filter to show equal loading of lysates. (**C**) Immunofluorescence of MCF-7 cells showing localization of GFP-Rab14 (green) and RFP-Nischarin (red) or RFP-Nischarin-NTD, as indicated. Bar: 10 μm. Plot showing extent of co-localization (as mean + s.d.) of fluorescence GFP-Rab14 and of RFP-Nischarin or RFP-Nischarin-NTD as measured by the Karl Pearson's coefficient of correlation. *P*-values were obtained with a Student's *t*-test comparing Nischarin with Nischarin-NTD ($n > 12$ cells per condition). (**D**) Immunofluorescence of MCF-7 cells showing localization of myc-Rac (mouse anti-myc antibody; secondary Alexa 647 anti-mouse antibody, green) and RFP-Nischarin (red) or RFP-Nischarin-NTD, as indicated. Bar: 10 μm. (**E**) Western blot analysis of HEK293T cell lysates containing full length or deletion constructs of myc-Nischarin before (total lysates, TL) and after incubation with GST-Rac in presence of either GDP or GMP∼PNP. (**F**) Immunofluorescence image of MCF-7 cells showing localization of myc-Rac1-Q61L (mouse anti-myc antibody; secondary Alexa 647 anti-mouse antibody, red), RFP-Nischarin (green) and GFP-Rab14 (blue). Scale bar = 10 μm.

Nischarin-CTD interacted only with the GTP-bound form of Rac1. Thus, it appears that Rac1 interacts with Nischarin at two distinct domains: inactive Rac1 with the NTD of Nischarin, active Rac1 with both the NTD and the CTD of Nischarin.

Since members of two different classes of small GTPases—Rac and Rab—bind to Nischarin, the question was whether this binding was mutually exclusive. Immunofluorescence revealed co-localization of RFP-Nischarin, myc-Rac1-Q61L

and GFP-Rab14 (Figure 2F), suggesting that a Nischarin dimer (Lim and Hong, 2004) may simultaneously bind Rac1 and Rab14. Alternatively, Nischarin dimers exclusively binding Rac or Rab14 are present on the same vesicle. Dimerization of Nischarin was confirmed by immunoprecipitation experiments using GFP-Nischarin and myc-Nischarin (Supplementary Figure S2C). These observations suggest that the shared effector Nischarin unites Rac and Rab14 mediated trafficking pathways.

Nischarin interacts with early and late endosomal Rab GTPases

Nischarin localizes to early, sorting and recycling endosomes but not to late endosomes or the Golgi (Supplementary Figure S3A; Lim and Hong, 2004). Rab14 localizes to a fraction of early endosomes and recycling endosomes and Golgi, but not to late endosomes (Supplementary Figure S3B; Junutula *et al*, 2004). Since Rab14 binds Nischarin, it is possible that Nischarin, like the two previously identified effectors of Rab14—Rabenosyn-5 and RUFY1/Rabip4 (Eathiraj *et al*, 2005; Yamamoto *et al*, 2010)—also participates in the early endosome/recycling pathway (Lim and Hong, 2004). Surprisingly, markers for various endosomal compartments revealed partial co-localization of Nischarin and GFP-Rab14 with the late endosome marker CD63 (LAMP-3), though GFP-Rab14 showed negligible co-localization with CD63 in the absence of Nischarin (Figure 3A). These observations suggest that the Nischarin-Rab14 complex may direct endocytic vesicles away from the early endosome/recycling pathway towards the late endosomal compartment possibly by interacting with other Rab GTPases localized on late endosomes.

A yeast two-hybrid analysis with 45 different Rab GTPases as bait to determine if other Rab GTPases interact with Nischarin (Figure 3B) identified three additional Rab GTPases—Rab4A, Rab9A and Rab38. Rab4 is the closest homologue of Rab14 (Junutula *et al*, 2004) but Rab9 and Rab38 are distantly related. Rab4, Rab14 and Rab9 are ubiquitously expressed, whereas Rab38 is almost exclusively expressed in melanocytes (Jäger *et al*, 2000). In addition, Rab38 failed to co-localize with Nischarin, as did the Rab38-Q69L mutant, which was completely cytosolic, suggesting a lack of prenylation (Supplementary Figure S3C). Interactions of Nischarin with Rab4 and Rab9 were confirmed in *in vitro* and cell-based experiments. GST bead binding of Nischarin to Rab4A and Rab9A was GTP dependent (Figure 3C), and involved the CTD of Nischarin; the same domain as used by Rab14 (Supplementary Figures S2A and S3D). FRAP analysis showed that Nischarin 'locks' Rab4 and Rab9 in a GTP-bound state on the membrane in living cells, as observed for Rab14 (Supplementary Figure S3E; Figure 3D). Moreover, expression of Nischarin in HEK293T cells resulted in an elevation in the membrane-bound pool while decreasing the cytosolic pool of Rab9 (Figure 3E). Immunofluorescence revealed that Nischarin co-localized with Rab4, Rab9 and GTP-locked forms Rab4-Q67L and Rab9-Q66L, but not with GDP-locked forms Rab4-S22N and Rab9-S21N (Supplementary Figure S3F; Figure 3F). Collectively, this suggests that Nischarin can be recruited to endosomes via its PX domain to interact with at least three different Rab GTPases that localize to different endosomal compartments.

Nischarin regulates the transition of Rab14 early endosomes to Rab9 late endosomes

We determined the localization of the Nischarin-Rab9 and Nischarin-Rab14 complexes in relation to the late endosomal/lysosomal marker CD63. Rab9 localized to CD63-containing late endosomes (Supplementary Figure S4A). Nischarin/CD63-positive structures were seen in almost all cells by immunofluorescence upon co-expression of Rab14, and especially Rab9 (Figures 3A and 4A). This was confirmed by immunoelectron microscopy of HEK293T cells: GFP-Nischarin localized poorly to LAMP-2-positive late endosomal/lysosomal compartments unless Rab9 or Rab14 was co-expressed (Figure 4B). Although Rab9 localized Nischarin to a CD63-positive compartment, these compartments did not label for Cathepsin D indicating that they do not represent lysosomes (Supplementary Figure S4B).

Since Rab4, Rab9 and Rab14 bind the same domain of Nischarin, the question was whether these Rab GTPases compete or collaborate for binding. We expressed various combinations of Rab GTPases and Nischarin in MCF-7 cells to determine co-localization. Expression of Rab9 affected the co-localization of Nischarin with Rab4 and Rab14, suggesting that Rab9 effectively competes with Rab4 and Rab14 for the Rab binding site of Nischarin with high efficiency *in vivo* (Supplementary Figure S4C; Figure 4C).

What are the functions of the different Rab–Nischarin complexes? Rab9 regulates transport of the cation-independent mannose 6-phosphate receptor (CI-MPR) from the late endosome to the trans-Golgi network and is involved in lysosome biogenesis (Lombardi *et al*, 1993; Riederer *et al*, 1994). Since Rab9 influences the total amount of CI-MPR present in the cell, we were interested in the effect of Nischarin on CI-MPR. Knockdown of Rab9 increased the total amount of CI-MPR as reported earlier (Ganley *et al*, 2004), while knockdown of Rab14 or Nischarin failed to change CI-MPR levels (Supplementary Figure S5A). This suggests that Rab14 and Nischarin, unlike Rab9, have no role in transport from late endosomes to the trans-Golgi network. We also observed a strong reduction in Rab9 upon Nischarin knockdown and vice versa, suggesting that similar to TIP47, Nischarin and Rab9 are dependent on each other for stability (Ganley *et al*, 2004; Supplementary Figure S5B). Stability can be considered as a read-out for interaction, and this observation suggests that Nischarin is an important effector for Rab9.

Maturation of Rab5 early endosomes into Rab7 late endosomes is controlled by timed recruitment of GAPs and GEFs where Rab5 controls Rab7 activation (Rink *et al*, 2005; Kinchen and Ravichandran, 2010; Poteryaev *et al*, 2010). Since Rab14 resides on early endosomal vesicles and Rab9 on late endosomal vesicles, and both Rab9 and Rab14 bind Nischarin, we speculated that Nischarin could regulate Rab14 to Rab9 transition of the vesicles and thereby affect progression from early to late endosomes. MCF7 cells with minimal or no endogenous expression of Nischarin were used to evaluate whether Nischarin can influence the co-localization of Rab14 and Rab9. In the absence of Nischarin, there was no co-localization, while the presence of Nischarin showed complete co-localization between Rab9 and Rab14 indicating that Nischarin plays an important role in bringing Rab9- and Rab14-positive endosomes together (Figure 4D). To further dissect the dynamics of transition from Rab14-positive endosomes to Rab9-positive endosomes, we

first studied the recruitment of Rab14 to early endocytic vesicles by following endocytosis of far-red microspheres in cells expressing GFP-Nischarin and RFP-Rab14. The rapid recruitment of Rab14 to a sub-population of endocytosed microspheres was followed by recruitment of Nischarin. During maturation, Rab14 was lost first, followed by the loss of Nischarin (Supplementary Movie 1; Figure 5A). Maturing vesicles are known to have progressively less PI(3)P (Lindmo and Stenmark, 2006), which may explain the loss of Nischarin. To investigate whether Rab14-positive endosomes eventually acquire Rab9, we expressed BFP-Rab9, GFP-Nischarin and RFP-Rab14 in A172 cells and timed their recruitment to maturing vesicles. Rab14-positive endosomes first recruited Nischarin, followed by progressive recruitment of Rab9, which continued while Nischarin was released from the vesicles (Supplementary Movie 2; Figure 5B and C). These results suggest that Nischarin is initially recruited to Rab14-positive early endosomes where it subsequently

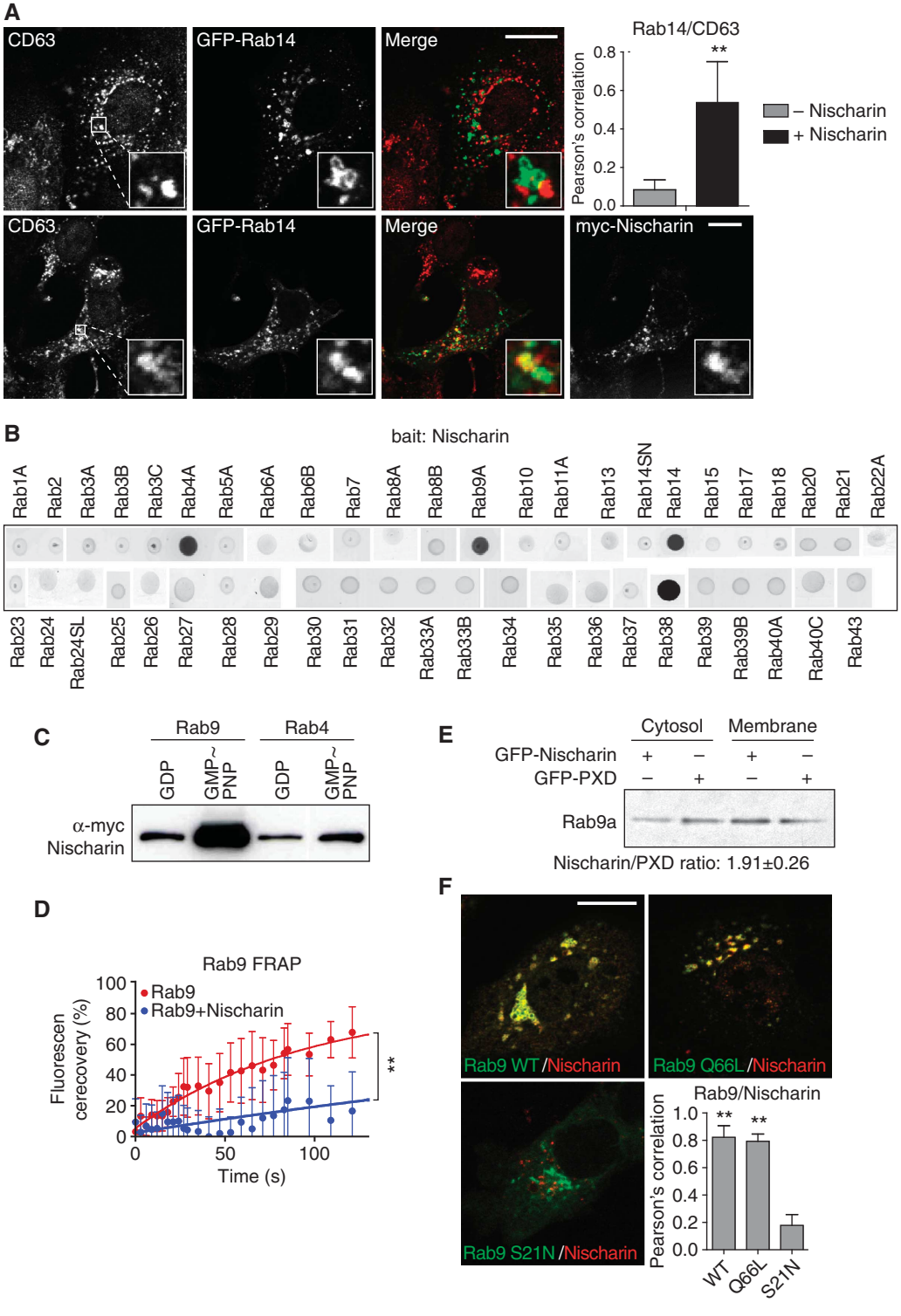

interacts with the late endosomal Rab9 to promote maturation of the endosome.

Recruitment of Nischarin to the SVC promotes survival of Salmonella

Regulation by Nischarin of two Rab GTPases acting on different endosomal compartments may contribute to the intracellular survival of *Salmonella* in SCVs. *Salmonella* has to enter acidified compartments such as late endosomes for propagation since a low pH induces the secretion of SPI-2 effector proteins which regulate SCV maintenance (Beuzón *et al*, 1999). Yet an SCV has to avoid fusion with lysosomes to prevent degradation of the pathogen (Rathman *et al*, 1996; Méresse *et al*, 1999). Many molecules capable of interacting with Nischarin are located on the SCV including PI(3)P, Rac1, Rab4, Rab14 and Rab9, of which some are known to regulate formation and maintenance of *Salmonella* SCVs (Hardt *et al*, 1998; Hernandez *et al*, 2004; Smith *et al*, 2007). As reported earlier (Bakowski *et al*, 2011), GFP-Rab14 was recruited to a subset of SCVs directly after cellular entry of *Salmonella* (Supplementary Movie 3; Figure 6A). Immunofluorescence of *Salmonella*-infected cells revealed that Nischarin was recruited to SCVs, where it accumulated during the first 5 h, and remained associated with the SCV for at least 16 h (Supplementary Figure S6A; Figure 6B and C). Whereas Rab14 associated with the SCV for <2 h (Supplementary Figure S6B), in agreement with the data published previously (Bakowski *et al*, 2011). Knockdown of Rab14 reduced recruitment of Nischarin to the SCV (Figure 6D). Knockdown of Rab9 also reduced recruitment of Nischarin by reducing either the total amount of Nischarin (Supplementary Figure S5B) or only the recruitment of Nischarin to SCV (Figure 6D).

The effect of Nischarin and its interacting partners on the fate of *Salmonella* in A172 cells was ascertained using a strain of *Salmonella* that expresses DsRed exclusively under low Mg^{2+} conditions of the intracellular environment of an SCV. Knockdown of Nischarin, Rab9, Rab14 or Rac1 by siRNA reduced intracellular growth of *Salmonella* during 18 h after infection of A172 cells (Supplementary Figure S6C; Figure 6E). This reduction indicates a role for of Nischarin and the three interacting GTPases in the survival of *Salmonella*. Knockdown of Rab7, which prevents maturation of the phagosome, was used as a positive control for reduced *Salmonella* proliferation (Méresse *et al*, 1999).

Survival and replication of *Salmonella* inside a host cell requires acidification of the SCV (Rathman *et al*, 1996) that precedes the step involving blockage of fusion of lysosomes with SCV. The early endosome to late endosome transition regulated by Nischarin may participate in maturation and acidification of the SCV. Indeed, knockdown of Nischarin and Rab7 in A172 cells led to a decrease in acidification of the SCV, which may explain the reduced bacterial load at 18 h post infection (Supplementary Figure S6D; Figure 6F).

If Nischarin is involved in controlling intracellular infections of bacterial pathogens such as *Salmonella*, then the question is whether it is expressed in the relevant cell types. When *Salmonella* enters the body through uptake via M cells in the gut, it first encounters macrophages and dendritic cells before coming into contact with other cell types. Quantitation of RNA expression by microarrays showed that Nischarin is expressed at higher levels in monocytes compared to the average for whole body expression (Supplementary Figure S6E). We therefore evaluated mRNA levels of Nischarin in THP-1 cells, a human acute monocytic leukaemia cell line, which can be differentiated into macrophages by phorbol 12-myristate-13-acetate (PMA) (Supplementary Figure S6F) and found these levels of Nischarin mRNA in THP-1 cells are comparable with those in A172 cells.

Reducing the amount of Nischarin in THP-1-derived macrophages by lentivirus-mediated knockdown showed a dose-dependent decrease in *Salmonella* load (Supplementary Figure S6G). Whereas human THP-1 cells (or any other human macrophages) are not permissive for replication of *Salmonella* (Bueno *et al*, 2008), mouse macrophages do allow for intracellular replication of *Salmonella*. The mouse macrophage cell line RAW264.7 expresses readily detectable amounts of Nischarin. Knockdown of Nischarin protein levels with siRNA in RAW264.7 macrophages proved ineffective, leading us to generate a zinc finger nuclease-based Nischarin knockout cells (generated by integration of GFP under a PGK promoter in exon 9 through homologues DNA-dependent repair at the zinc finger restriction site; Supplementary Figure S7A and B). Nischarin knockout reduced the bacterial load in infected cells by $\sim$25% upon 18 h post infection (Figure 6G). Moreover, the knockout cells showed a clear reduction in acidification of the SCV, indicating that Nischarin plays a role during SCV maturation in biologically relevant host cells (Figure 6H).

Figure 3 Nischarin bridges early and late endosomal Rab GTPases. (**A**) Co-localization and quantification of GFP-Rab14-Q70L (green) with CD63 (rabbit-anti-CD63 antibody; secondary Alexa 568 anti-rabbit antibody; red) in the presence or absence of ectopically expressed myc-Nischarin (mouse-anti-myc antibody; secondary Alexa 647 anti-mouse antibody; blue). Scale bar = 10 μm. The upper right plot depicts extent of co-localization (as mean + s.d.) of fluorescence of CD63 and GFP-Rab14 as measured by the Karl Pearson's coefficient of correlation. *P*-values were obtained with a Student's *t*-test ($n>12$ cells per condition). (**B**) Nischarin binds multiple endosomal Rab GTPases (Rab4, Rab9, Rab14 and Rab 38). Yeast two-hybrid analysis of prey Nischarin-CTD and as bait 45 GTP-locked forms (active site Gln to Leu substitution) of Rab GTPases along with a negative control of Rab14 GDP-bound form (Rab14-S25N). Both wild-type and S67L variant of Rab24 were included. (**C**) GST bead-binding assay of myc-Nischarin incubated with GST-Rab9A or GST-Rab4A in the presence of GDP or GMP$\sim$PNP. Bound material was separated by SDS–PAGE and the western blot was probed with anti-myc antibody. (**D**) Fluorescent recovery curves after photobleaching of GFP-Rab9A expressed in MCF-7 cells in the presence or absence of ectopically expressed Nischarin, as indicated. The data shown is the mean ± s.d. of at least seven individual FRAP experiments. *P*-values were obtained with F-test comparing FRAP curves of Rab9 with Rab9 + Nischarin. (**E**) Fractionated membrane and cytosol of HEK293T cells expressing Nischarin or PX domain of Nischarin (GFP–PX) were separated by SDS–PAGE. The western blot was probed for endogenous Rab9 with anti-Rab9 antibody. The membrane cytosol ratio of cells expressing Nischarin was divided by the membrane cytosol ratio of cells expressing the PX domain (two independent experiments). (**F**) Co-localization and quantification of myc-Nischarin (mouse-anti-myc antibody; secondary Alexa 647 anti-mouse antibody; red) with GFP-Rab9-WT; GTP-locked GFP-Rab9-Q66L; and GDP-locked Rab9-S21N. Scale bar = 10 μm. The lower right plot shows extent of co-localization (as mean + s.d.) of fluorescence of Nischarin and Rab9-WT, Rab9-Q66L and Rab9-S21N as measured by the Karl Pearson's coefficient of correlation. *P*-values were obtained with a Student's *t*-test comparing Rab9-S21N with Rab9-WT or Rab9-Q66L ($n>12$ cells per condition).

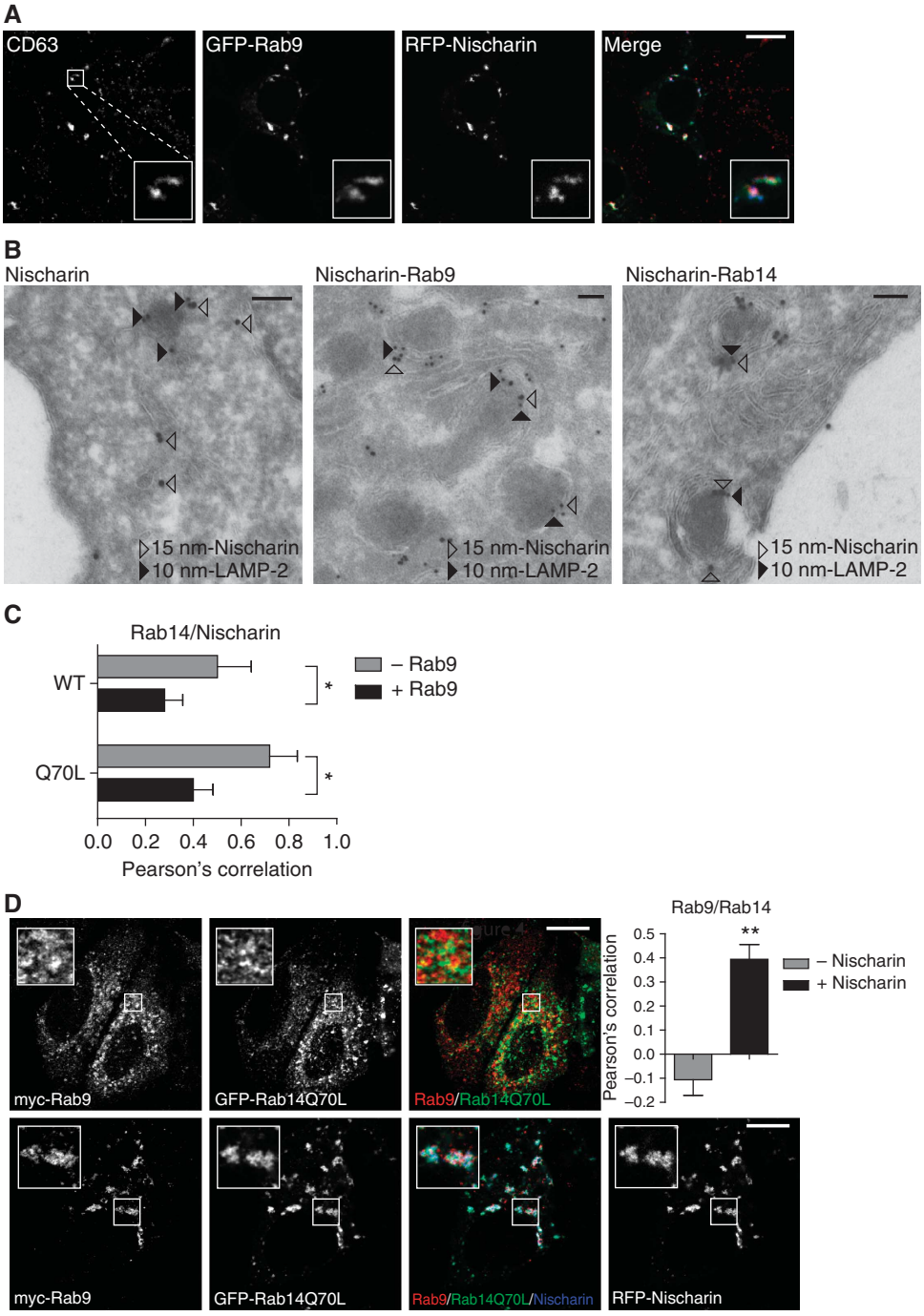

Figure 4 Nischarin together with Rab9/14 localizes to late endosomes but not to lysosomes. (**A**) Co-localization of GFP-Rab9 (green) and RFP-Nischarin (blue) with endogenous CD63. A172 cells are stained with mouse-anti-CD63 and secondary Alexa 647 anti-mouse (red). Scale bar = 10 μm. (**B**) Immunoelectron micrograph of T-REx (HEK293T derived) cells stably expressing GFP-Nischarin with or without RFP-Rab9/14, labelled with rabbit anti-GFP (15 nm gold) and mouse anti-LAMP-2 (10 nm gold). Scale bar = 100 nm. (**C**) Fluorescence microscopy was used to quantify co-localization of RFP-Nischarin with WT or GTP-locked forms of GFP-Rab14 expressed in MCF-7 cells in the presence or absence of ectopically expressed Rab9. Plot depicts extent of co-localization (as mean + s.d.) between fluorescence of Nischarin, GFP-Rab14 and GFP-Rab14-Q70L in the presence and absence of ectopic Rab9 expression as measured by the Karl Pearson's coefficient of correlation. *P*-values were obtained with a Student's *t*-test comparing Rab14 co-localization with Nischarin in the presence or absence of Rab9 ($n > 12$ cells per condition). (**D**) Co-localization and quantification of GFP-Rab14-Q70L (green) with myc-Rab9 (mouse-anti-myc antibody; secondary Alexa 647 anti-mouse antibody; red) in the presence or absence of ectopically expressed RFP-Nischarin (blue). Scale bar = 10 μm. One representative experiment out of two is shown. The data shown in the plot represents the average of >5 cells per condition. The variation in co-localization is depicted as standard deviations. *P*-value was obtained with a Student's *t*-test comparing Rab14 co-localization with Rab9 in the presence or absence of Nischarin.

Discussion

Since small GTPases orchestrate the formation, transport and fusion of endocytic vesicles, we wished to explore their role in the formation of *Salmonella*-containing vesicles (SCV) for intracellular proliferation of *Salmonella*. A total of 18 different Rab GTPases are known to associate with SCVs at some point during their formation and maturation; some of these Rab GTPases may directly regulate formation and

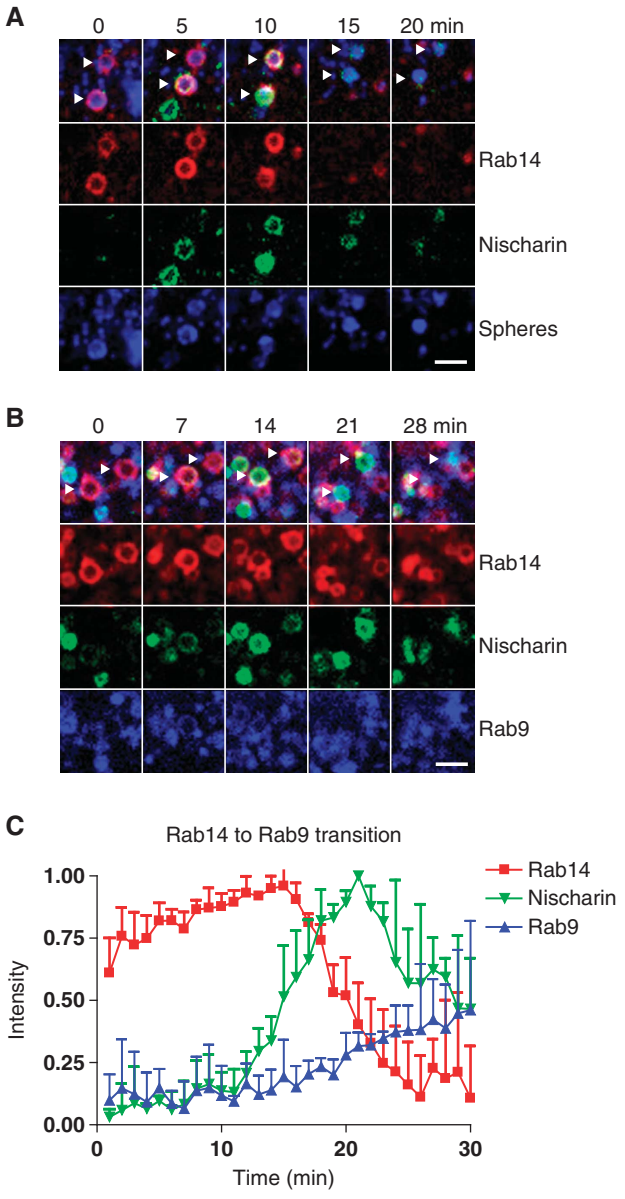

Figure 5 Nischarin regulates transition of Rab14 early endosomes to Rab9 late endosomes. (**A**) Rab14 recruits Nischarin to Rab14-positive endosomes. A172 cells transfected with RFP-Rab14 (red), GFP-Nischarin (green) constructs and loaded with 660 nm FluoSpheres (blue) for 10 min followed by live-cell imaging for 30 min. Images shown are from time-laps movie depicting Rab14, Nischarin-positive endosomes at various time intervals. Arrowheads point to vesicles that sequentially recruit Rab14 and Nischarin. Scale bar = 4 μm. (**B**) Nischarin converts Rab14-positive endosomes to Rab9-positive endosomes. A172 cells transfected with RFP-Rab14 (red), GFP-Nischarin (green) and BFP-Rab9 (blue) constructs. After 24 h transfection, live-cell imaging was carried out for 30 min. Arrowheads point to endosomes that sequentially recruit Rab14, Nischarin and Rab9. Scale bar = 4 μm. (**C**) Quantification of 10 vesicles from time laps movies. All vesicle intensity traces were aligned to the peak intensity present in the Nischarin trace. Error bars depict standard deviation.

maintenance of SCVs (Brumell and Scidmore, 2007). Here, we have identified a novel Rac and Rab GTPase dual effector—Nischarin—that interacts serially with Rac and Rab14/9 GTPases in the course of vesicle maturation and affects intracellular *Salmonella* survival.

The CTD of Nischarin, along with its PI(3)P binding domain, participates in targeting Nischarin to Rab14-positive endosomes. Though neither endogenous Nischarin nor endogenous Rab14 individually localize to late endosomes, co-expression of these proteins (and perhaps Rab4 as well) localizes them to acidified Rab9-positive late endosomes. Depletion of functional Nischarin from either glioblastoma (A172) cells or macrophages decreases acidification of the SCV and a resultant decrease in *Salmonella* replication. Based on these observations, we propose a model for the action of Nischarin in facilitating survival of *Salmonella* in SCVs (Figure 7). As per this model, Nischarin may be recruited to early endosomes (phagosomes) via its interaction with Rac GTPase or binding to PI(3)P via its PX domain. In the next stage of formation of SCVs, Nischarin locates to SCVs by interacting with Rab14 via its CTD. Nischarin then recruits Rab9 on endocytic vesicles concomitant with acidification of the SCV, and thereby creates a compartment wherein *Salmonella* are rendered competent for replication.

This model is supported by various observations. Rac GTPase is activated on early endosomes in a Rab5-dependent process (Baust *et al*, 2006; Palamidessi *et al*, 2008). The presence of Rac on endosomes might explain the recruitment of Nischarin to this compartment; in addition, Rab5 stimulates the local production of PI(3)P on early endosomes (Christoforidis *et al*, 1999), which may facilitate direct binding of Nischarin. Since *Salmonella* also stimulates PI(3)P production on SCVs (Mallo *et al*, 2008), conditions are favourable for recruitment of Nischarin to this compartment. Regarding the role of Rab14, this GTPase has been shown to be recruited to the SCV (Kuijl *et al*, 2007) and to promote *Salmonella* survival. Rab14 has also been shown to be recruited to phagosomes that contain *Mycobacterium tuberculosis* and block maturation of these vesicles into phagolysosomes (Kyei *et al*, 2006). Finally, Rab9 was shown to be recruited to the SCV and *Salmonella*-induced filaments (SIFs). The expression of a dominant-negative mutant of Rab9 inhibits the formation of SIFs (Smith *et al*, 2007).

In addition, the SopE and SopB effectors secreted by *Salmonella* activate not only small GTPases, but also Akt and p21-activated kinases 3 and 4 (PAK3 and PAK4). PAK3 and PAK4 have previously been shown to interact with Nischarin (Chen *et al*, 1999; Steele-Mortimer, 2000; Alahari *et al*, 2004; Kuijl *et al*, 2007). PAK3 also interacts directly with activated Rac GTPase and mediates downstream signalling and actin remodelling while PAK4, which is activated downstream of Akt, also regulates actin remodelling (Manser *et al*, 1994; Wells *et al*, 2002; Kuijl *et al*, 2007). Rab14 is activated indirectly by Akt by the phosphorylation and subsequent inactivation of the Rab14 GAP protein AS160 (Larance *et al*, 2005; Mîinea *et al*, 2005; Stöckli *et al*, 2008). The fact that at least two (PAK and Rac) out of the four (PAK, Rac, IRS4 and Integrin-α5) previously known interaction partners of Nischarin and two (Rab14 and Rab9) out of the three Rab GTPases identified in this study are all activated during infection by *Salmonella* suggests that this pathogen can hijack Nischarin to modulate vesicular trafficking/fusion. We have shown by expression profiling that Nischarin is highly expressed in macrophages/dendritic cells, which are among the first cell types that *Salmonella* colonizes upon passage through intestinal M cells. We have also shown that a

complete knock-out of Nischarin in RAW264.7 macrophages attenuates intracellular *Salmonella* replication, adding support for a relevant role for Nischarin during *Salmonella* infection.

Nischarin may also be involved in signalling pathways. Nischarin interacts with the IRS4—a player in insulin receptor signalling (Sano *et al*, 2002)—and has been identified as a component in downstream signalling of the ephrin receptor EphB2 (Darie *et al*, 2011). Akt, PAK, Erk and Rac, all of which are activated upon *Salmonella* entry, are also activated by Receptor Tyrosine Kinases. Since all these proteins are either directly or indirectly affect Nischarin, it is

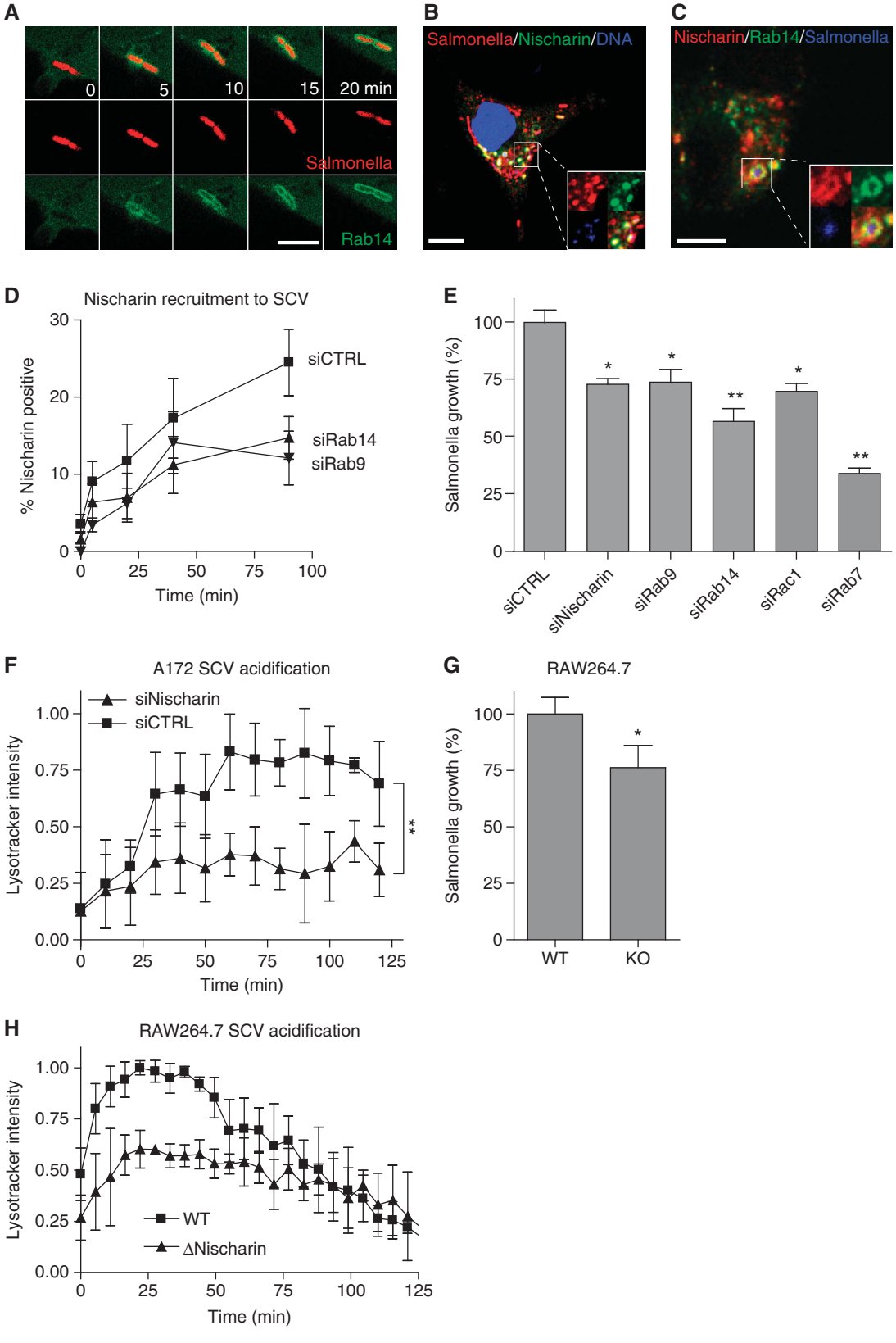

possible that Nischarin may act as an adaptor molecule of receptor tyrosine kinases that mediate downstream signalling and receptor trafficking events.

In an uninfected cell, the co-localization of Nischarin with Rab GTPases on early and late endosomes is consistent with a role in the control of the endo-phagosomal maturation process in a mode parallel to, or in combination with the Rab5 to Rab7 conversion model (Rink *et al*, 2005; Kinchen and Ravichandran, 2010; Poteryaev *et al*, 2010). During maturation of phagosomes and vesicles from a early to late endosomes, the amount of PI(3)P decreases, creating a concentration gradient of this molecule (Yeung and Grinstein, 2007). PI(3)P is essential for membrane recruitment of Nischarin through its PX domain. Although late endosomes contain lower amounts of PI(3)P, they do contain more Rab9 for which Nischarin has higher affinity. The combination of these factors could drive the maturation of a Rab14-positive early endosome to a Rab9-positive late endosome. Nischarin may be released from the Rab9-containing late endosomes due to depletion of PI(3)P; this may then free Rab9 to bind to other effectors. Thus, a Nischarin-mediated pathway may be one of several mechanisms controlling the timing of maturation of endosomes and phagosomes.

The study of bacterial pathogen–host interactions is fraught with complexity of both host and bacterial biology, and their interplay. Nevertheless, studies of host–pathogen interactions can elaborate the normal function of host proteins, which the pathogens modify or exploit to their own benefit. Here, we have shown Nischarin to be an effector protein that interacts with multiple members of Rac and the Rab GTPase family; this dual effector protein that may control endosome maturation is exploited by *Salmonella* to promote its survival and replication inside host vesicles. Further research will reveal if Nischarin is involved in the survival of just *Salmonella* (and possibly *Mycobacteria*), or in the pathology of many other (or all) intracellular pathogens.

Materials and methods

Reagents

Generation and affinity purification of Rabbit anti-Rab14 antibodies were described earlier (Junutula *et al*, 2004). Nischarin rabbit polyclonal antibodies were raised against GST-PXD (aa 11–118) and affinity purified against MBP-PXD (aa 11–118). Antibodies were dialysed against PBS and stored in the presence of 40% glycerol at −80°C. Other antibodies used were Rabbit polyclonal and monoclonal anti-CD63 antibody (Vennegoor *et al*, 1985), mouse monoclonal anti-Nischarin antibody (BD Biosciences, San Jose, CA), Mouse anti-HA epitope tag antibody (3F10, Roche Diagnostics, Indianapolis, IN), Mouse anti-myc epitope tag antibody (9E10, Covance, Emeryville, CA) and polyclonal anti-cathepsin D antibody (Millipore, Billerica, MA). Anti-Rab9 was obtained from Cell Signalling (D52G8, Danvers, MA). Mouse anti-Rac was obtained from Upstate (Lake Placid, NY), Mouse monoclonal anti-EEA1 antibody (BD Biosciences), Rat anti-LAMP2 (ABL-93; Santa Cruz Biotechnology, Santa Cruz, CA) and Goat anti-EEA1 (N-19; Santa Cruz Biotechnology). Goat anti-mouse, Goat anti-Rabbit, Donkey anti-Rat and Donkey anti-Goat antibodies (conjugated with Alexa 405, 488, 594 or 647 dye), Zenon tricolor kit (Green, Orange and Deep Red), FluoSpheres 660 of 0.04 μm and lysotracker red (DND-99) were purchased from Invitrogen (Carlsbad, CA). Anti-GFP antibodies, mouse brain cDNA yeast two-hybrid library and reagents related to yeast two-hybrid screening were purchased from Clontech Laboratories (Palo Alto, CA).

cDNA constructs and vectors

Described in Supplementary data.

Cell culture

MCF-7, PC12, HEK293T, T-Rex (HEK293T derived), RAW264.7 and A172 cells were maintained in complete DMEM (Invitrogen). THP-1 cells were maintained in complete RPMI-1640. Additional details for transfection and differentiation are described in Supplementary data.

Yeast two-hybrid screen

Rab14-Q70L$_{\Delta C}$ was cloned into pGBKT7. The screen was performed using the 'MATCHMAKER GAL4 Two-Hybrid System 3' according to manufactures protocol with the mouse brain cDNA yeast two-hybrid library from Clontech Laboratories.

Yeast two-hybrid assay

Competent yeast cells were co-transformed with 1–2 μg each of bait and prey plasmid DNA. Doubly transformed yeast cells were selected by plating on leucine and tryptophan double dropout media on SD-agar plates. Fully grown double positive yeast colonies were patched on quadruple selection SD-agar plates where leucine, tryptophan, histidine and adenine were dropped out from the media. Cells were able to grow on this medium only if a protein–protein interaction between the bait and prey proteins allowed expression of the corresponding reporter proteins.

Figure 6 Recruitment of Nischarin to the SVC promotes survival of *Salmonella*. (**A**) Co-localization of GFP-Rab14 (green) and DsRED-*Salmonella* (red) in MCF-7 cells. Scale bar = 4 μm. (**B**) Immunofluorescence of endogenous Nischarin (Rabbit-anti-Nischarin, secondary Alexa 488 anti-rabbit antibody, green) and *Salmonella* (Rabbit-anti-*Salmonella* directly conjugated to Alexa 647) in A172 cells. DNA is counterstained with HCS NuclearMask blue stain (blue). Scale bar = 10 μm. (**C**) Co-localization of endogenous Rab14 (rabbit anti-Rab14 antibody, secondary Alexa 488 anti-rabbit antibody, green) and endogenous Nischarin (mouse anti-Nischarin antibody, secondary Alexa 647 anti-mouse antibody, red) in PC12 cells infected with sBFP2-*Salmonella* (blue). Scale bar = 10 μm. (**D**) Quantification by fluorescence microscopy of recruitment of endogenous Nischarin in A172 cells to the SCV in the presence or absence of siRNA mediated knockdown of Rab9 or Rab14. One representative experiment out of two was shown. The data shown in the plot is the average of eight positions per condition (>100 bacteria per time point). The variation in Nischarin levels is depicted as standard deviations of the eight positions in a given experimental condition. (**E**) Quantification of intracellular growth of DsRed-*Salmonella* in A172 cells treated with siRNA to knockdown expression of Nischarin, Rab9, Rab14, Rac1 and control siRNA (siCTRL) by FACS. Plot shows extent of *Salmonella* proliferation (as mean + s.d.) normalized to siCTRL. *P*-values were obtained with a Student's *t*-test comparing all samples to siCTRL ($n = 3$ experiments). (**F**) Quantification of SCV acidification in A172 cells measured by accumulation of lysotracker red in the SCV. A172 treated with siCTRL or siNischarin cells were infected with GFP-expressing *Salmonella* in the presence of lysotracker red. Images were taken at time points indicated and the intensity of lysotracker red fluorescence in SCVs was quantified. Average of three experiments (>100 bacteria per time point) is shown. (**G**) Quantification of intracellular growth of DsRed-*Salmonella* in RAW264.7 cells and RAW264.7 Nischarin knockout cells by FACS. Plot shows *Salmonella* proliferation (as mean + s.d.) normalized to wild-type (WT) cells. *P*-values were obtained with a Student's *t*-test comparing knockout samples to wild type ($n = 3$ experiments). (**H**) Quantification of SCV acidification in RAW264.7 macrophages measured by accumulation of lysotracker red in the SCV. RAW264.7 or RAW264.7 Nischarin knockout cells were infected with BFP-expressing *Salmonella* in the presence of lysotracker red. Images were taken at time points indicated and the intensity of lysotracker red fluorescence in SCVs was quantified. One representative experiment out of two was shown. The data shown in the plot is the average of four positions per condition (>100 bacteria per time point). The variation in lysotracker levels is depicted as standard deviations of the four positions in a given experimental condition.

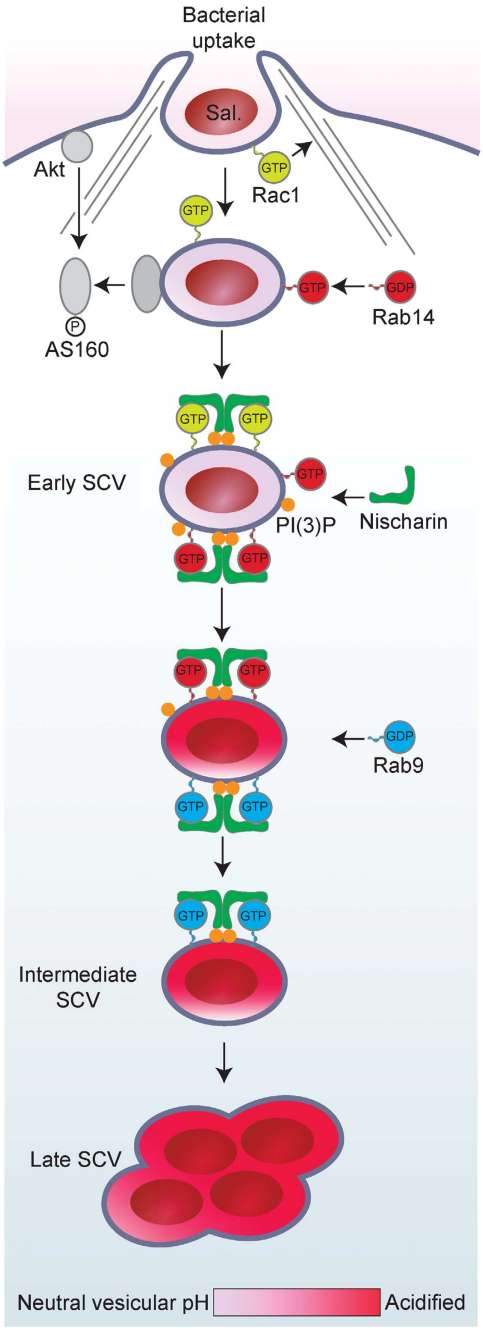

Figure 7 Model for maturation of the SCV in the presence of Nischarin. The *Salmonella* T3SS effector SopE activates Rac1 and regulates actin dynamics during entry. The effector SopB induces the production of PI(3)P on the phagosome and activates Akt, inactivating AS160, keeping Rab14 active allowing for the recruitment of Nischarin. Nischarin binds PI(3)P and the small GTPases Rac1, Rab14 and Rab9. The sequential binding of Nischarin with Rab14 and Rab9 GTPases where Nischarin plays an important role in transitioning Rab14-positive endosomes to Rab9-positive endosomes thereby promoting endosome maturation and the acidification of the SCV and as a consequence the intracellular survival of *Salmonella*. Sal. denotes *Salmonella*. The roles of grey coloured proteins in the model are from the published literature.

Expression and purification of recombinant proteins

Recombinant GST-Rab and Rac constructs were transformed into *E. coli* BL21 (DE3) or BL21-Codon Plus (DE3)-RIL cells. Expression and purification details are described in Supplementary data.

Exchange of bound nucleotides in Rab proteins with GMP∼PNP/GDP

GST-fusion proteins were incubated in nucleotide exchange buffer containing GDP or GMP∼PNP (100 μM) for 20 min at room temperature. The bound nucleotides were stabilized by incubation in nucleotide stabilization buffer. Additional details are described in Supplementary data.

GST bead-binding assay

HEK293T cell lysates from transfected cells were incubated with glutathione-agarose beads for 1 h to pre-clear the lysate. Pre-cleared lysates were allowed to bind to GST-Rab-glutathione-agarose at 4°C for 1 h. The beads were washed five times with ice-cold PBS. Bound proteins were eluted with 50 μl of SDS sample loading buffer and analysed by SDS–PAGE and western blotting. Please see Supplementary data for further details.

Immunoprecipitations

Described in Supplementary data.

Fractionation of proteins according to cellular location

HEK293T cells were transfected with GFP-Nischarin or PX domain of Nischarin (GFP-Nischarin-PXD). Transfection efficiency was >80% as evaluated by eye. The Qproteome Cell Compartment Kit (QIAGEN, Valencia, CA) was used according to manufactures protocol. Protein content of all fractions was quantified with BCA and equal amounts of protein were separated by SDS–PAGE followed by western blotting.

Microscopy

Images were taken with a Leica microscope (TCS-SP1, TCS-SP2 or AOBS) equipped with HCX Plan-Apochromat ×63NA 1.32 and HCX Plan-Apochromat lbd.bl ×63NA 1.4 oil-corrected objective lenses (Leica Microsystems, Wetzlar, Germany), Zeiss AxioObserver Z1 CCD microscope equipped with a ×40/0.7 Plan-Neofluar objective and a Hamamatsu ORCA-ER camera, or Nikon Eclipse TE2000-U (inverted) equipped with a CSU 21 Yokogawa spinning disk head. Additional details are described in Supplementary data.

Immunoelectron microscopy

Described in Supplementary data.

Fluorescence recovery after photobleaching

MCF-7 cells expressing GFP-Rab14, GFP-Rab9A or GFP-Rab4A molecules were mounted for microscopy (Leica AOBS) without fixing and exposed to a laser beam to bleach the fluorescence associated with a single vesicle. The microscope contains a 37°C humidified 5% CO_2 culture chamber for culturing and imaging the cells. The cells were monitored over 120 s to follow and quantify the exchange of bleached Rab GTPase molecules on the vesicle by fluorescent Rab GTPases from the cytosol. Because vesicles were not completely stationary during the course of the experiment, their positions were manually tracked by a program written in Matlab (Mathworks, Natick, MA). For each curve at least seven vesicles were measured.

Bacterial strains, growth conditions and infections

Plasmid pMW215 or pMW211 expressing DsRED was a kind gift from Dirk Bumann, Infection Biology Biozentrum, University of Basel. sBFP2 (Kremers *et al*, 2007) was a kind gift from Theodorus WJ Gadella, Swammerdam Institute for Life Sciences, University of Amsterdam. Codon optimized tagBFP was ordered from geneART GMBH, Regensburg, Germany. The mouse-virulent strains *Salmonella enterica* serovar typhimurium SL1344 and GFP (plasmid pFPV 25.1; Cormack *et al*, 1996) were a kind gift from Stephan Meresse, Centre d'Immunologie de Marseille-Luminy. Please see Supplementary data for further details on the gentamycin protection assay used for infection.

SCV acidification

A172 or RAW264.7 cells were infected for 10 min with tagBFP-*Salmonella*. After infection, lysotracker red and anti-*Salmonella* antibodies directly conjugated to Alexa 647 were added to the culture supernatant. The lysotracker intensity was measured in

the SCV, excluding extracellular bacteria (labelled with the anti-*Salmonella* antibody).

Image analysis

Co-localization of fluorescent tags was measured with WCIF_ imageJ package and the co-localization plugin. Quantification of membrane markers on the SCV was performed with Cellprofiler (Carpenter *et al*, 2006). Bacteria were identified as primary objects. The primary object was dilated with two pixels to form a secondary object. The primary object was subtracted from the secondary object to yield the phagosomal membrane area. The average intensity of the fluorescent molecule (e.g., Rab) was measured within this area. Lysotracker red was measured in the primary object.

Microarray data

Described in Supplementary data.

Statistical analysis

Statistical analysis was performed in Graphpad Prism. *T*-test analysis was done with two tails and equal variance. FRAP and acidification data were fitted with the one site binding (hyberbola) equation and tested for similarity using the F-test and error bars represent standard deviations. Co-localization was determined on a per cell basis with the Karl Pearson's correlation coefficient as measurement. Images of cells were derived from multiple experiments ($n \geqslant 3$), unless otherwise indicated. *P*-values <0.05 are indicated with a single asterisk and *P*-values <0.01 are indicated with a double asterisk.

qPCR

Described in Supplementary data.

Lentiviral production

The TRC-2 (shRNA scrambled control) and TRC-256839 shNischarin were packed with MISSION Lentiviral Packaging mixture from Sigma-Aldrich (St Louis, MO) in HEK293 cells according to manufacturer's protocol. Lentiviral particles were concentrated using Lenti-X concentrator from Clontech. Concentrated virus was added in serial dilutions to THP-1 cells (1:4, 1:16 and 1:64) in the presence of 6 μg/ml polybrene.

Zinc finger knockout

Zinc finger nucleases targeting mouse Nischarin (target site: TACCTGGACCTGAGTCACAATGGACTGCGAGTTGTGGAT) were ordered from Sigma-Aldrich. A plasmid containing homology 920 nt upstream and 834 nt downstream of the predicted cleavage site was ordered from genewiz (South Plainfield, NJ). GFP under a pgk promoter was cloned at the expected cleavage site. DNA (2 μg) of each zinc finger nuclease and 3 μg of linear DNA containing the homology arms and pgk-GFP were transfected into RAW264.7 via electroporation. After 7 days, GFP-positive cells (~1%) were singe cell sorted (two 96-well plates) and after 4 weeks tested for Nischarin expression via immunofluorescence. Eight percent of GFP-positive single cell clones had a complete knockout of Nischarin protein as confirmed by immunofluorescence staining using anti-Nischarin antibodies. Nischarin knockout cells were further analysed for any defects in LAMP2 and EEA1 staining. Two knockout clones (2D6 and 2F7) and two wild-type clones (1G10 and 1G12, with pgk-GFP integration) were used in all further experiments.

Supplementary data

Supplementary data are available at *The EMBO Journal* Online (http://www.embojournal.org).

Acknowledgements

We thank Dr Vidya Jonnalagadda for critical reading and editing of the manuscript and Raj J Advani for the help with yeast two-hybrid screening. We thank Dr Eric Brown and Dr Vishva Dixit for crucial feedback and insightful discussions. We thank Dr Dirk Buman for the DsRed plasmid pMW215 and Prof. Dr TWJ Gadella for the SBFP2 plasmid and Dr Stéphan Méresse for *Salmonella* strains. MP acknowledges Genentech and CIEE (Council on International Educational Exchange) for sponsoring his graduate research program at Genentech, Inc. and CSIR for the graduate fellowship at Osmania University. SJ acknowledges support from UGC-SAP/DRS-II and is thankful for Genentech for 'Visiting Scientist' opportunity. Research grants to SKA were supported by NIH (5RO1CA115706) and to HJ and JN were supported by NWO-TOP and an ERC Adv grant.

Author contributions: CK, MP, SKA and JRJ designed and performed the experiments. HJ, PK and KEE performed the experiments. MC and SJ helped with experiments. RH and JN provided guidance on experimental design. CK and JRJ wrote the paper.

Conflict of interest

CK, PK and MC are (or were) either graduate visiting Student's/postdoctoral employees of Genentech, Inc. and KEE, RHS and JRJ are full time employees of Genentech, Inc. at the time this work was conducted.

References

Alahari SK, Nasrallah H (2004) A membrane proximal region of the integrin alpha5 subunit is important for its interaction with nischarin. *Biochem J* **377:** 449–457

Alahari SK, Reddig PJ, Juliano RL (2004) The integrin-binding protein Nischarin regulates cell migration by inhibiting PAK. *EMBO J* **23:** 2777–2788

Bakowski MA, Braun V, Lam GY, Yeung T, Heo WD, Meyer T, Finlay BB, Grinstein S, Brumell JH (2011) The phosphoinositide phosphatase SopB manipulates membrane surface charge and trafficking of the salmonella-containing vacuole. *Cell Host Microbe* **7:** 453–462

Baust T, Czupalla C, Krause E, Bourel-Bonnet L, Hoflack B (2006) Proteomic analysis of adaptor protein 1A coats selectively assembled on liposomes. *Proc Natl Acad Sci USA* **103:** 3159–3164

Beuzón CR, Banks G, Deiwick J, Hensel M, Holden DW (1999) pH-dependent secretion of SseB, a product of the SPI-2 type III secretion system of Salmonella typhimurium. *Mol Microbiol* **33:** 806–816

Brumell JH, Scidmore MA (2007) Manipulation of rab GTPase function by intracellular bacterial pathogens. *Microbiol Mol Biol Rev* **71:** 636–652

Bueno SM, González PA, Carreño LJ, Tobar JA, Mora GC, Pereda CJ, Salazar-Onfray F, Kalergis AM (2008) The capacity of Salmonella to survive inside dendritic cells and prevent antigen presentation to T cells is host specific. *Immunology* **124:** 522–533

Carpenter AE, Jones TR, Lamprecht MR, Clarke C, Kang IH, Friman O, Guertin DA, Chang JH, Lindquist RA, Moffat J, Golland P, Sabatini DM (2006) CellProfiler: image analysis software for identifying and quantifying cell phenotypes. *Genome Biol* **7:** R100

Chen LM, Bagrodia S, Cerione RA, Galán JE (1999) Requirement of p21-activated kinase (PAK) for Salmonella typhimurium-induced nuclear responses. *J Exp Med* **189:** 1479–1488

Christoforidis S, Miaczynska M, Ashman K, Wilm M, Zhao L, Yip SC, Waterfield MD, Backer JM, Zerial M (1999) Phosphatidylinositol-3-OH kinases are Rab5 effectors. *Nat Cell Biol* **1:** 249–252

Cormack BP, Valdivia RH, Falkow S (1996) FACS-optimized mutants of the green fluorescent protein (GFP). *Gene* **173:** 33–38

Darie CC, Deinhardt K, Zhang G, Cardasis HS, Chao MV, Neubert TA (2011) Identifying transient protein-protein interactions in EphB2 signaling by Blue Native PAGE and Mass Spectrometry. *Proteomics* **11:** 4514–4528

Drecktrah D, Knodler LA, Howe D, Steele-Mortimer O (2007) Salmonella trafficking is defined by continuous dynamic interactions with the endolysosomal system. *Traffic* **8:** 212–225

Eathiraj S, Pan X, Ritacco C, Lambright DG (2005) Structural basis of family-wide Rab GTPase recognition by rabenosyn-5. *Nature* **436:** 415–419

Ganley IG, Carroll K, Bittova L, Pfeffer S (2004) Rab9 GTPase regulates late endosome size and requires effector interaction for its stability. *Mol Biol Cell* **15:** 5420–5430

Garcia-del Portillo F, Finlay BB (1995) Targeting of Salmonella typhimurium to vesicles containing lysosomal membrane glycoproteins bypasses compartments with mannose 6-phosphate receptors. *J Cell Biol* **129:** 81–97

Garcia-del Portillo F, Zwick MB, Leung KY, Finlay BB (1993) Intracellular replication of Salmonella within epithelial cells is associated with filamentous structures containing lysosomal membrane glycoproteins. *Infect Agents Dis* **2:** 227–231

Haraga A, Ohlson MB, Miller SI (2008) Salmonellae interplay with host cells. *Nat Rev Microbiol* **6:** 53–66

Hardt WD, Chen LM, Schuebel KE, Bustelo XR, Galán JE (1998) S. typhimurium encodes an activator of Rho GTPases that induces membrane ruffling and nuclear responses in host cells. *Cell* **93:** 815–826

Hensel M, Shea JE, Waterman SR, Mundy R, Nikolaus T, Banks G, Vazquez-Torres A, Gleeson C, Fang FC, Holden DW (1998) Genes encoding putative effector proteins of the type III secretion system of Salmonella pathogenicity island 2 are required for bacterial virulence and proliferation in macrophages. *Mol Microbiol* **30:** 163–174

Hernandez LD, Hueffer K, Wenk MR, Galán JE (2004) Salmonella modulates vesicular traffic by altering phosphoinositide metabolism. *Science* **304:** 1805–1807

Jefferies HBJ, Cooke FT, Jat P, Boucheron C, Koizumi T, Hayakawa M, Kaizawa H, Ohishi T, Workman P, Waterfield MD, Parker PJ (2008) A selective PIKfyve inhibitor blocks PtdIns(3,5)P(2) production and disrupts endomembrane transport and retroviral budding. *EMBO Rep* **9:** 164–170

Jones BD, Ghori N, Falkow S (1994) Salmonella typhimurium initiates murine infection by penetrating and destroying the specialized epithelial M cells of the Peyer's patches. *J Exp Med* **180:** 15–23

Jordens I, Fernandez-Borja M, Marsman M, Dusseljee S, Janssen L, Calafat J, Janssen H, Wubbolts R, Neefjes J (2001) The Rab7 effector protein RILP controls lysosomal transport by inducing the recruitment of dynein-dynactin motors. *Curr Biol* **11:** 1680–1685

Junutula JR, De Maziére AM, Peden AA, Ervin KE, Advani RJ, van Dijk SM, Klumperman J, Scheller RH (2004) Rab14 is involved in membrane trafficking between the Golgi complex and endosomes. *Mol Biol Cell* **15:** 2218–2229

Jäger D, Stockert E, Jäger E, Güre AO, Scanlan MJ, Knuth A, Old LJ, Chen YT (2000) Serological cloning of a melanocyte rab guanosine 5'-triphosphate-binding protein and a chromosome condensation protein from a melanoma complementary DNA library. *Cancer Res* **60:** 3584–3591

Kinchen JM, Ravichandran KS (2010) Identification of two evolutionarily conserved genes regulating processing of engulfed apoptotic cells. *Nature* **464:** 778–782

Kohbata S, Yokoyama H, Yabuuchi E (1986) Cytopathogenic effect of Salmonella typhi GIFU 10007 on M cells of murine ileal Peyer's patches in ligated ileal loops: an ultrastructural study. *Microbiol Immunol* **30:** 1225–1237

Kremers G-J, Goedhart J, van den Heuvel DJ, Gerritsen HC, Gadella TWJ (2007) Improved green and blue fluorescent proteins for expression in bacteria and mammalian cells. *Biochemistry* **46:** 3775–3783

Kuijl C, Savage NDL, Marsman M, Tuin AW, Janssen L, Egan DA, Ketema M, van den Nieuwendijk R, van den Eeden SJF, Geluk A, Poot A, van der Marel G, Beijersbergen RL, Overkleeft H, Ottenhoff THM, Neefjes J (2007) Intracellular bacterial growth is controlled by a kinase network around PKB/AKT1. *Nature* **450:** 725–730

Kyei GB, Vergne I, Chua J, Roberts E, Harris J, Junutula JR, Deretic V (2006) Rab14 is critical for maintenance of Mycobacterium tuberculosis phagosome maturation arrest. *EMBO J* **25:** 5250–5259

Larance M, Ramm G, Stöckli J, van Dam EM, Winata S, Wasinger V, Simpson F, Graham M, Junutula JR, Guilhaus M, James DE (2005) Characterization of the role of the Rab GTPase-activating protein AS160 in insulin-regulated GLUT4 trafficking. *J Biol Chem* **280:** 37803–37813

Lim K-P, Hong W (2004) Human Nischarin/imidazoline receptor antisera-selected protein is targeted to the endosomes by a combined action of a PX domain and a coiled-coil region. *J Biol Chem* **279:** 54770–54782

Lindmo K, Stenmark H (2006) Regulation of membrane traffic by phosphoinositide 3-kinases. *J Cell Sci* **119:** 605–614

Lombardi D, Soldati T, Riederer MA, Goda Y, Zerial M, Pfeffer SR (1993) Rab9 functions in transport between late endosomes and the trans Golgi network. *EMBO J* **12:** 677–682

Lostroh CP, Lee CA (2001) The Salmonella pathogenicity island-1 type III secretion system. *Microbes Infect* **3:** 1281–1291

Mallo GV, Espina M, Smith AC, Terebiznik MR, Alemán A, Finlay BB, Rameh LE, Grinstein S, Brumell JH (2008) SopB promotes phosphatidylinositol 3-phosphate formation on Salmonella vacuoles by recruiting Rab5 and Vps34. *J Cell Biol* **182:** 741–752

Manser E, Leung T, Salihuddin H, Zhao ZS, Lim L (1994) A brain serine/threonine protein kinase activated by Cdc42 and Rac1. *Nature* **367:** 40–46

McGhie EJ, Brawn LC, Hume PJ, Humphreys D, Koronakis V (2009) Salmonella takes control: effector-driven manipulation of the host. *Curr Opin Microbiol* **12:** 117–124

Méresse S, Steele-Mortimer O, Finlay BB, Gorvel JP (1999) The rab7 GTPase controls the maturation of Salmonella typhimurium-containing vacuoles in HeLa cells. *EMBO J* **18:** 4394–4403

Mîinea CP, Sano H, Kane S, Sano E, Fukuda M, Peränen J, Lane WS, Lienhard GE (2005) AS160, the Akt substrate regulating GLUT4 translocation, has a functional Rab GTPase-activating protein domain. *Biochem J* **391:** 87–93

Palamidessi A, Frittoli E, Garré M, Faretta M, Mione M, Testa I, Diaspro A, Lanzetti L, Scita G, Di Fiore PP (2008) Endocytic trafficking of Rac is required for the spatial restriction of signaling in cell migration. *Cell* **134:** 135–147

Pavlova B, Volf J, Ondrackova P, Matiasovic J, Stepanova H, Crhanova M, Karasova D, Faldyna M, Rychlik I (2011) SPI-1-encoded type III secretion system of Salmonella enterica is required for the suppression of porcine alveolar macrophage cytokine expression. *Vet Res* **42:** 16

Pfeffer S (2003) Membrane domains in the secretory and endocytic pathways. *Cell* **112:** 507–517

Poteryaev D, Datta S, Ackema K, Zerial M, Spang A (2010) Identification of the switch in early-to-late endosome transition. *Cell* **141:** 497–508

Rathman M, Sjaastad MD, Falkow S (1996) Acidification of phagosomes containing Salmonella typhimurium in murine macrophages. *Infect Immun* **64:** 2765–2773

Reddig PJ, Xu D, Juliano RL (2005) Regulation of p21-activated kinase-independent Rac1 signal transduction by nischarin. *J Biol Chem* **280:** 30994–31002

Rescigno M, Urbano M, Valzasina B, Francolini M, Rotta G, Bonasio R, Granucci F, Kraehenbuhl JP, Ricciardi-Castagnoli P (2001) Dendritic cells express tight junction proteins and penetrate gut epithelial monolayers to sample bacteria. *Nat Immunol* **2:** 361–367

Riederer MA, Soldati T, Shapiro AD, Lin J, Pfeffer SR (1994) Lysosome biogenesis requires Rab9 function and receptor recycling from endosomes to the trans-Golgi network. *J Cell Biol* **125:** 573–582

Rink J, Ghigo E, Kalaidzidis Y, Zerial M (2005) Rab conversion as a mechanism of progression from early to late endosomes. *Cell* **122:** 735–749

Sano H, Liu SCH, Lane WS, Piletz JE, Lienhard GE (2002) Insulin receptor substrate 4 associates with the protein IRAS. *J Biol Chem* **277:** 19439–19447

Smith AC, Heo WD, Braun V, Jiang X, Macrae C, Casanova JE, Scidmore MA, Grinstein S, Meyer T, Brumell JH (2007) A network of Rab GTPases controls phagosome maturation and is modulated by Salmonella enterica serovar Typhimurium. *J Cell Biol* **176:** 263–268

Souwer Y, Griekspoor A, Jorritsma T, de Wit J, Janssen H, Neefjes J, van Ham SM (2009) B cell receptor-mediated internalization of salmonella: a novel pathway for autonomous B cell activation and antibody production. *J Immunol* **182:** 7473–7481

Steele-Mortimer O (2000) Activation of Akt/Protein Kinase B in Epithelial Cells by the Salmonella typhimurium Effector SigD. *J Biol Chem* **275:** 37718–37724

Steele-Mortimer O, Méresse S, Gorvel JP, Toh BH, Finlay BB (1999a) Biogenesis of Salmonella typhimurium-containing vacuoles in epithelial cells involves interactions with the early endocytic pathway. *Cell Microbiol* **1:** 33–49

Steele-Mortimer O, Méresse S, Gorvel JP, Toh BH, Finlay BB (1999b) Biogenesis of Salmonella typhimurium-containing vacuoles in epithelial cells involves interactions with the early endocytic pathway. *Cell Microbiol* **1:** 33–49

Stöckli J, Davey JR, Hohnen-Behrens C, Xu A, James DE, Ramm G (2008) Regulation of glucose transporter 4 translocation by the Rab guanosine triphosphatase-activating protein AS160/TBC1D4: role of phosphorylation and membrane association. *Mol Endocrinol* **22:** 2703–2715

Vennegoor C, Calafat J, Hageman P, van Buitenen F, Janssen H, Kolk A, Rümke P (1985) Biochemical characterization and cellular localization of a formalin-resistant melanoma-associated antigen reacting with monoclonal antibody NKI/C-3. *Int J Cancer* **35:** 287–295

Wells CM, Abo A, Ridley AJ (2002) PAK4 is activated via PI3K in HGF-stimulated epithelial cells. *J Cell Sci* **115:** 3947–3956

Yamamoto H, Koga H, Katoh Y, Takahashi S, Nakayama K, Shin H-W (2010) Functional cross-talk between Rab14 and Rab4 through a dual effector, RUFY1/Rabip4. *Mol Biol Cell* **21:** 2746–2755

Yeung T, Grinstein S (2007) Lipid signaling and the modulation of surface charge during phagocytosis. *Immunol Rev* **219:** 17–36

Yu X-J, McGourty K, Liu M, Unsworth KE, Holden DW (2010) pH sensing by intracellular Salmonella induces effector translocation. *Science* **328:** 1040–1043

Zerial M, McBride H (2001) Rab proteins as membrane organizers. *Nat Rev Mol Cell Biol* **2:** 107–117